Available online at www.sciencedirect.com
SCIENCE DIRECT®
Journal of Solid State Chemistry 178 (2005) 3284–3292
JOURNAL OF SOLID STATE CHEMISTRY
www.elsevier.com/locate/jssc

Synthesis and Eu^{3+} luminescence in new oxysilicates, $ALa_3Bi(SiO_4)_3O$ and $ALa_2Bi_2(SiO_4)_3O$ [A=Ca, Sr and Ba] with apatite-related structure

N. Lakshminarasimhan, U.V. Varadaraju*

Materials Science Research Centre and Department of Chemistry, Indian Institute of Technology Madras, Chennai 600 036, India

Received 10 February 2005; received in revised form 25 May 2005; accepted 14 August 2005
Available online 15 September 2005

Abstract

New oxysilicates with the general formula $ALa_3Bi(SiO_4)_3O$ and $ALa_2Bi_2(SiO_4)_3O$ [A=Ca, Sr and Ba] are synthesized and characterized. Powder X-ray diffraction of these silicates show that they are isostructural with $BiCa_4(VO_4)_3O$ which has an apatite-related structure. Eu^{3+} luminescence in the newly synthesized oxysilicates show broad emission lines due to disorder of cations. The relatively high intense magnetic dipole transition $^5D_0 \rightarrow {}^7F_1$ points to a more symmetric environment. The photoluminescence results confirm that the compounds have apatite-related crystal structure.

Keywords: Apatite; Silicate; Bi^{3+}; Powder X-ray diffraction; IR spectroscopy; Photoluminescence; Eu^{3+}

1. Introduction

Apatites comprise a large family of isostructural compounds with the general formula $A_5(TO_4)_3X$ where A is a large divalent cation (Ca^{2+}, Sr^{2+}, Pb^{2+}, Cd^{2+}, etc.), TO_4 is a trivalent anionic group (PO_4^{3-}, VO_4^{3-}, AsO_4^{3-}, etc.) and X is a monovalent anion (F^-, Cl^-, OH^-, etc.). The compound $Ca_5(PO_4)_3F$ is a representative of apatite family. It crystallizes in the space group $P6_3/m$ [1]. The free anion X^- is surrounded by three A^{2+} cations (forming a triangle). The X^- anion positions itself in the plane of the triangle. However, depending on the size of the X^- anion, there occurs a deviation in the position of X from the plane of the triangle. This leads to minor deviations in the crystal structure. For instance, the apatite $Ca_5(PO_4)_3Cl$ where X is Cl^- crystallizes in the monoclinic space group $P2_1$ and $Ca_{10-x}Eu_x(PO_4)_6S_{1+x/2}$ where X is S^{2-} in the hexagonal space group $P6_3$ [2,3]. Sansom et al. have shown from neutron diffraction studies that the compounds $La_{9.33}Si_6O_{26}$ and $La_8Sr_2Si_6O_{26}$ crystallize in hexagonal cell with space group P-3 [4]. The large divalent A cation can be substituted by trivalent cations such as rare earth ions and the charge neutrality is maintained by simultaneous substitution of either trivalent anionic group by tetravalent anionic group or monovalent X anion by divalent anion as given by

$$A^{2+} + TO_4^{3-} = A^{3+} + TO_4^{4-},$$

$$A^{2+} + X^- = A^{3+} + X^{2-}.$$

Apatites find potential application as bioceramics, luminescent host lattices, etc. [5,6]. In recent times, considerable attention is paid to the rare earth containing silicate and germanate apatites with the general formula $RE_{9.33}(TO_4)_6O_2$ [T=Si and Ge] due to their high oxide ion conductivity [4,7]. The silicate apatites are known for the past three decades. Ito reported a wide range of rare earth containing silicate oxyapatites with the general formula $A_2RE_8(SiO_4)_6O_2$ where A is a divalent cation (Mg, Ca, Sr, Ba, Cd, Pb and Mn) and RE is a trivalent rare earth ion (La, Nd, Sm, Gd, Dy, Er and Y) [8]. Felsche reported rare earth silicates of the formula $RE_{9.33}\square_{0.67}(SiO_4)_6O_2$ (where $\square$ is vacancy), $LiRE_9(SiO_4)_6O_2$, $NaRE_9(SiO_4)_6O_2$, $A_2RE_8(SiO_4)_6O_2$ [A=Mg, Ca, Sr and Ba] and $A_4RE_6(SiO_4)_6(OH)_2$ [A=Ca, Sr, Ba and Pb] where RE=La–Lu, and found that they all have apatite structure [9]. Eu^{3+} luminescence has been reported in silicate oxyapatites

*Corresponding author. Fax: 91 44 2257 0509.
E-mail address: varada@iitm.ac.in (U.V. Varadaraju).

0022-4596/$ - see front matter © 2005 Elsevier Inc. All rights reserved.
doi:10.1016/j.jssc.2005.08.006

$Ca_2RE_8(SiO_4)_6O_2$ [RE=La, Gd and Y] and $Mg_2RE_8(SiO_4)_6O_2$ [RE=La and Y] [10]. Blasse has proposed a model to predict the site occupancy of cations in apatite structure based on local charge compensation and this model was substantiated by the Eu^{3+} emission results obtained by Isaacs in silicate oxyapatites [10,11]. Blasse explained the high intensity of $^5D_0 \rightarrow {}^7F_0$ transition in La analogues as due to the presence of smaller Eu^{3+} in 6 h site of apatite structure where the coordination of Eu^{3+} by a free oxygen is possible and in Y analogues, Eu^{3+}, being bigger than Y^{3+}, occupies 4*f* site where such free oxygen is absent.

Not much is known about Bi^{3+} containing apatites in the literature. A review on the crystal chemistry of apatites covering 74 chemically distinct apatite compounds shows only one Bi^{3+} containing apatite, $BiCa_4(VO_4)_3O$ [12]. $BiCa_4(VO_4)_3O$ has been reported to have apatite-related structure [13]. Due to the presence of $6s^2$ lone pair of electrons, Bi^{3+} substitution leads to a distortion in the Ca site resulting in three different Ca sites, Ca(1), Ca(2) and Ca(3). This results in the loss of mirror plane and the space group thus changes from ideal $P6_3/m$ to $P6_3$. Similarly the phosphate analogues $BiCa_4(PO_4)_3O$ and $LaCa_4(PO_4)_3O$ have been reported more recently [14]. Eu^{3+} luminescence has been used as a local structure probe in understanding the preferential occupancy of Bi^{3+} in irregular hexacoordinated Ca(2) site [15]. More recently, it is reported that Bi doping in germanate apatites lowers the synthesis and sintering temperatures [16]. The objective of the present study is to synthesize and characterize Bi^{3+} containing oxysilicate apatites with the general formula $ALa_3Bi(SiO_4)_3O$ and $ALa_2Bi_2(SiO_4)_3O$ [*A*=Ca, Sr and Ba] and to study Eu^{3+} luminescence in these silicates.

2. Experimental

2.1. Synthesis

All the compounds in the series $ALa_3Bi(SiO_4)_3O$ and $ALa_2Bi_2(SiO_4)_3O$ [*A*=Ca, Sr and Ba] were synthesized by high-temperature solid-state reaction method. The starting materials used were $CaCO_3$ (Cerac, 99.95%), $SrCO_3$ (Cerac, 99.99%), $BaCO_3$ (Cerac, 99.99%), La_2O_3 (Indian Rare Earths, 99.9%), Bi_2O_3 (Cerac, 99.9%) and SiO_2 (Thermal Syndicate, 99.9%). Stoichiometric amounts of the reactants were ground well and heated in a covered alumina crucible at 700 °C/12 h, 950 °C/24 h and 1250 °C/24 h with intermittent grindings. Eu^{3+} substituted compositions were synthesized using Eu_2O_3 (Indian Rare Earths, 99.9%). Eu^{3+} was substituted for La^{3+} with a concentration of 0.05 moles [$ALa_{2.95}Eu_{0.05}Bi(SiO_4)_3O$ and $ALa_{1.95}Eu_{0.05}Bi_2(SiO_4)_3O$].

2.2. Characterization

Phase identification of all the synthesized compounds was carried out by powder X-ray diffraction (XRD) using Cu-$K_{\alpha 1}$ radiation (P3000, Rich Seifert). The theoretical XRD patterns were generated using LAZY PULVERIX program [17]. The atomic coordinates used were that of $BiCa_4(VO_4)_3O$ [13]. The lattice parameters were calculated using least-squares fitting of high angle reflections. FT-IR spectra were recorded using KBr pellet technique (Spectrum One, Perkin-Elmer). Photoluminescence spectra of Eu^{3+} were recorded using a spectrofluorometer (FP-6500 Jasco) operating in the range 220–720 nm. All the spectra were recorded at room temperature. The excitation source was a 150 W Xenon lamp. Each spectrum was corrected for the baseline.

3. Results and discussion

3.1. Phase formation

Powder XRD patterns of the compositions are shown in Figs. 1 and 2. All the reflections could be indexed based on the theoretical pattern generated using LAZY PULVERIX program. The powder XRD patterns show highly crystalline phases. The reflections are fitted based on a hexagonal unit cell with space group $P6_3$. It is reported that the systematic absences for apatite phases with space group $P6_3/m$ and the oxyapatite $BiCa_4(VO_4)_3O$ with space group $P6_3$ are the same [13].

The calculated hexagonal '*a*' and '*c*' lattice parameters are listed in Table 1. Both '*a*' and '*c*' lattice parameters of $ALa_3Bi(SiO_4)_3O$ and $ALa_2Bi_2(SiO_4)_3O$ compounds show an increase with change of alkaline earth ion from Ca to Ba due to the increase in size. A comparison of the lattice parameters of $ALa_3Bi(SiO_4)_3O$ compounds with $ALa_2Bi_2(SiO_4)_3O$ compounds shows a marginal decrease in the lattice parameters for the latter compound and this is due to the substitution of bigger La^{3+} (1.06 Å) by smaller Bi^{3+} (1.02 Å). The variation in lattice parameters with alkaline earth ion in $ALa_3Bi(SiO_4)_3O$ and $ALa_2Bi_2(SiO_4)_3O$ is shown in Fig. 3. The variation in both '*a*' and '*c*' lattice parameters is nonlinear. A similar behaviour is reported for $BiCa_{4-x}Sr_x(PO_4)_3O$ [$x = 0-4$] [14]. In apatites with space group $P6_3/m$, substitutions at the 6 h lattice site result in the variation in the '*a*' axis [9]. Substitutions at the 4*f* site do not affect the '*a*' axis since shorter bonds of 6 h site lie in the directions [*hk*0]. It is also reported that the variation in '*c*' lattice parameter depends on the substitutions at the 4*f* site. The crystal structure of $BiCa_4(VO_4)_3O$ with space group $P6_3$ is close to that of apatite. The $Ca(1)O_6$ and $Ca(3)O_9$ polyhedra share faces forming a linear chain along '*c*' axis. These chains are interconnected by VO_4 tetrahedra in the ab plane. The $Ca(2)O_6$ polyhedra share corners with each other and form a chain along '*c*' axis. This suggests that substitution at any one of the sites will reflect on the variation of both '*a*' and '*c*' lattice parameters and accounts for the observed lattice parameter variation in $ALa_3Bi(SiO_4)_3O$ and $ALa_2Bi_2(SiO_4)_3O$ [*A*=Ca, Sr and Ba]. The nonlinear variation could be due to preferential occupancy of alkaline earth ions over the sites in the lattice.

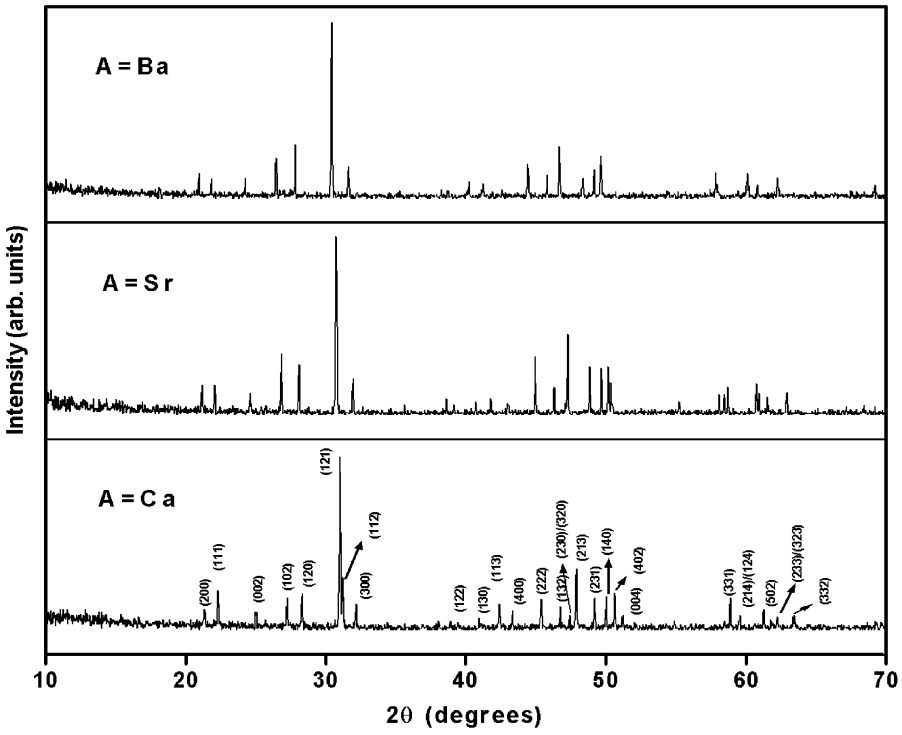

Fig. 1. Powder XRD patterns of ALa$_3$Bi(SiO$_4$)$_3$O [A=Ca, Sr and Ba].

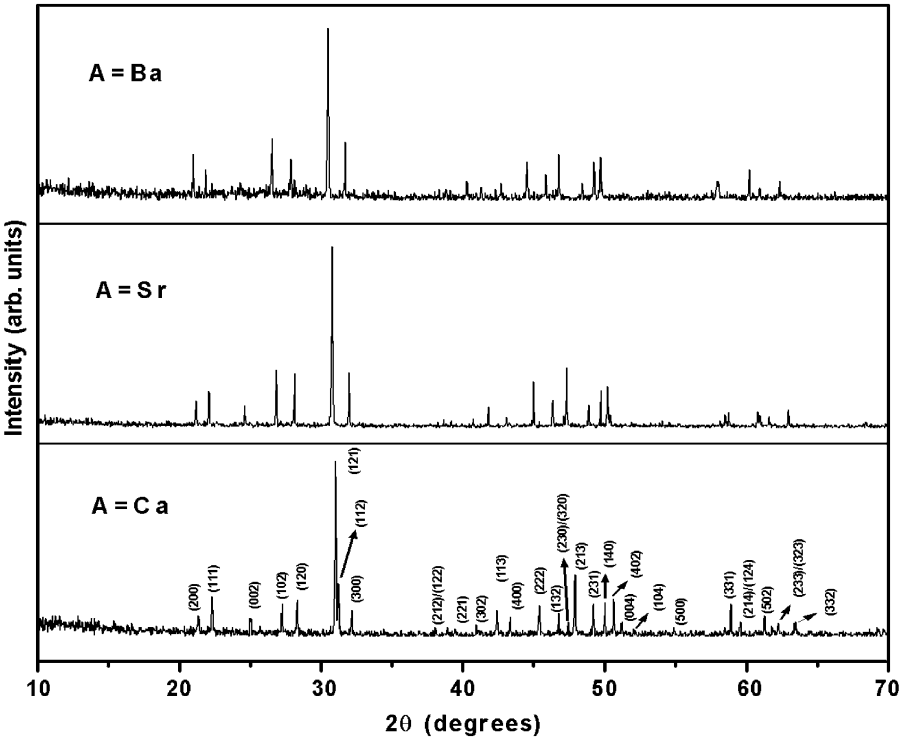

Fig. 2. Powder XRD patterns of ALa$_2$Bi$_2$(SiO$_4$)$_3$O [A=Ca, Sr and Ba].

3.2. FT-IR spectroscopy

FT-IR spectra of the synthesized ALa$_3$Bi(SiO$_4$)$_3$O and ALa$_2$Bi$_2$(SiO$_4$)$_3$O [A=Ca, Sr and Ba] compounds are shown in Figs. 4 and 5 respectively. Table 2 shows the IR spectral assignments for the compounds in the range 1200–450 cm^{-1}. The observed band at ~910 cm^{-1} is due to the stretching vibrations of SiO$_4$ group and the bands observed at around 490 and 530 cm^{-1} are due to the

bending vibrations of SiO_4 group [18]. These bands confirm the presence of orthosilicate group. It has been reported that the bands observed at 924–962 and 499–542 cm^{-1} are due to the asymmetric stretching and bending vibrations of SiO_4 group, respectively in $Ca_4La_6(SiO_4)_6O\square$; ($\square$ = vacancy) [19]. The broadness observed in the absorption peaks could be due to minor distortions in the SiO_4 group from ideal T_d symmetry. A similar broadness in the absorption bands of $-PO_4$ group has been reported by us for Bi^{3+} rich compositions in $Bi_{1-x}Eu_xCa_4(PO_4)_3O$ [$x = 0.1$, 0.3, 0.5, 0.8 and 1.0] and the reason for this has been attributed to the presence of $6s^2$ lone pair electrons of Bi^{3+} [15]. Based on this, the observed broadness in the absorption bands in the present study could be attributed to the distortions in SiO_4 group. These distortions are due to the presence of $6s^2$ lone pair electrons of Bi^{3+}. From Table 2, it is clear that both stretching and bending vibrations show a shift towards lower wavenumbers when the alkaline earth ion is changed from Ca to Ba in $ALa_3Bi(SiO_4)_3O$ and $ALa_2Bi_2(SiO_4)_3O$. This shift is due to the increase in size and mass of the alkaline earth ion as the alkaline earth ions are coordinated to the oxygen of SiO_4 group. It is reported that the absorption band observed at 539 cm^{-1} in $Ca_{10-x}Nd_x(PO_4)_{6-x}(SiO_4)_x(OH)_2$ corresponds to the Nd–O bond [20]. In our results, a shoulder is observed in Sr and Ba analogues at ~580 cm^{-1} and this can be attributed to La–O bond stretching.

Table 1
Hexagonal lattice parameters of $ALa_3Bi(SiO_4)_3O$ and $ALa_2Bi_2(SiO_4)_3O$

Compound	a (Å)	c (Å)
$CaLa_3Bi(SiO_4)_3O$	9.641(7)	7.134(7)
$SrLa_3Bi(SiO_4)_3O$	9.695(6)	7.230(6)
$BaLa_3Bi(SiO_4)_3O$	9.787(7)	7.329(7)
$CaLa_2Bi_2(SiO_4)_3O$	9.630(7)	7.110(7)
$SrLa_2Bi_2(SiO_4)_3O$	9.689(6)	7.229(6)
$BaLa_2Bi_2(SiO_4)_3O$	9.772(7)	7.317(7)

3.3. Photoluminescence studies

The photoluminescence excitation spectra of Eu^{3+} in $ALa_{2.95}Eu_{0.05}Bi(SiO_4)_3O$ and $ALa_{1.95}Eu_{0.05}Bi_2(SiO_4)_3O$ are shown in Figs. 6 and 7, respectively. The excitation spectra show a broad band in the region between 250 and 350 nm in all compounds and this is the Eu^{3+}–O^{2-} charge transfer band (CTB). It is known that Bi^{3+} absorption and Eu^{3+} CT absorption are observed in the UV region in many oxides [21]. Thus an overlap between Bi^{3+} and Eu^{3+} absorption is possible and this could result in the broadness of Eu^{3+}–O^{2-} CTB observed in the present study. The CTB is weak in the case of Ba analogues. The excitation of Eu^{3+} occurs from the ground $^7F_0$ level to various higher levels of Eu^{3+} and all the levels are labelled in the excitation spectra. The $^7F_0 \rightarrow {}^5L_6$ line at 395 nm is the strongest line in the excitation spectra.

Photoluminescence emission spectra of Eu^{3+} in $ALa_3Bi(SiO_4)_3O$ and $ALa_2Bi_2(SiO_4)_3O$ under 395 nm excitation are shown in Figs. 8 and 9 respectively. The overall

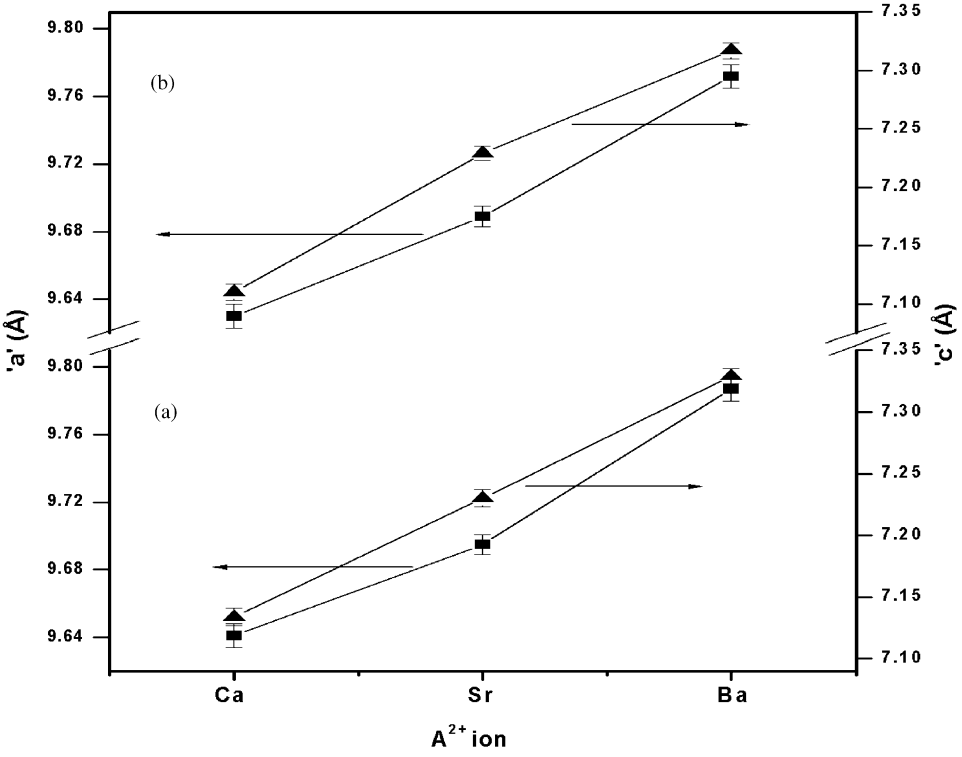

Fig. 3. Variation in 'a' [■] and 'c' [▲] lattice parameters with alkaline earth ion in (a) $ALa_3Bi(SiO_4)_3O$ and (b) $ALa_2Bi_2(SiO_4)_3O$ [A=Ca, Sr and Ba].

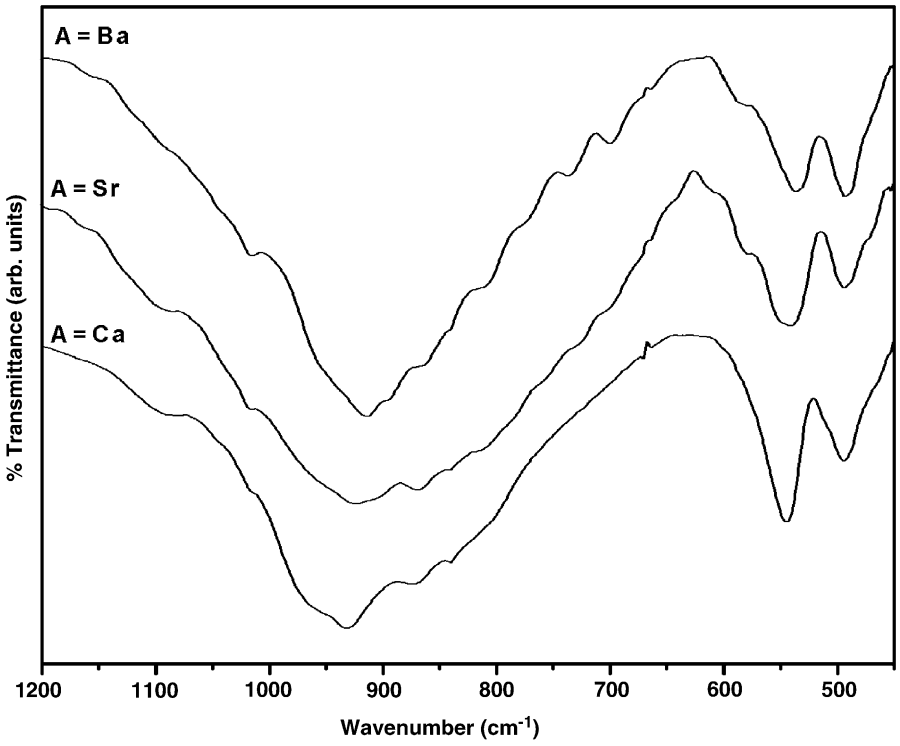

Fig. 4. FT-IR spectra of $A La_3Bi(SiO_4)_3O$ [A=Ca, Sr and Ba].

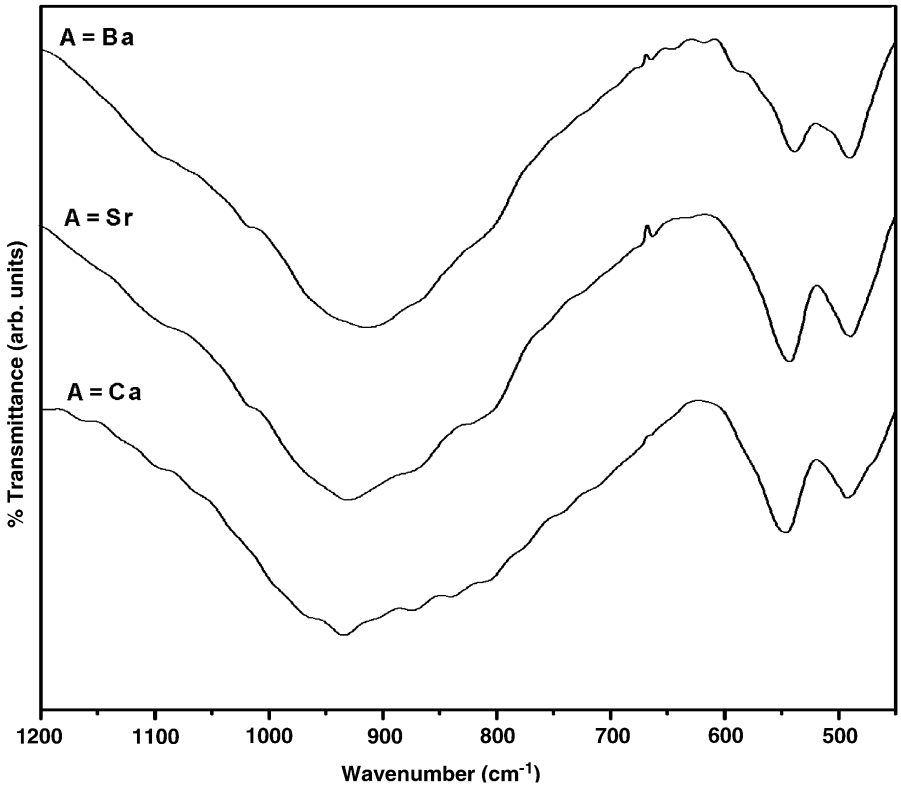

Fig. 5. FT-IR spectra of $ALa_2Bi_2(SiO_4)_3O$ [A=Ca, Sr and Ba].

emission features are same in all these compounds. The emission lines are the well-known $^5D_0 \rightarrow {}^7F_j$ ($j = 0, 1, 2$) transitions of Eu^{3+}. No emission from higher levels of $^5D_1$ and $^5D_2$ is observed. The reason for this is the non-radiative decay to $^5D_0$ level by multiphonon relaxation process that is favoured by the presence of high frequency

vibrations of the host lattice ($\nu_{SiO_4} = 930\,cm^{-1}$). The observed emission lines are broad. It is known that broad emission lines are expected when the crystal field at the Eu^{3+} ion differs from Eu^{3+} ion to Eu^{3+} ion due to variation in the surroundings [22]. Broad emission of Eu^{3+} reveals the disorder of cations in the crystal structure. Based on the broad emission lines of Eu^{3+} in $Ba_3Gd_2WO_9$, a perovskite oxide, it has been concluded that ordering of Gd^{3+} and W^{6+} is not complete [23]. Boyer et al. have observed broad emission line for Eu^{3+} in $Ca_2La_{7.8}Eu_{0.2}(SiO_4)_6O_2$ and from selective excitation in $^5D_0$ level it has been found that Eu^{3+} is distributed in two kinds of sites [24]. Similarly the broad emission lines of Eu^{3+} in $ALa_3Bi(SiO_4)_3O$ and $ALa_2Bi_2(SiO_4)_3O$ [A=Ca, Sr and Ba] suggest that there is a disorder of alkaline earth, La^{3+} and Bi^{3+} ions.

The emission spectra show the high intense line at 590 nm which is due to magnetic dipole $^5D_0 \rightarrow {}^7F_1$ transition. The emission line observed at 615 nm is the electric dipole transition, $^5D_0 \rightarrow {}^7F_2$. Figs. 8 and 9 show that in all three compounds, the magnetic dipole transition is the high intense line. The magnetic dipole transition becomes the high intense line when the site has a centre of symmetry [25]. In the present study, the high intense magnetic dipole transition shows the site is more symmetric. A similar behaviour is reported in $La_{0.95}Eu_{0.05}Ca_4(PO_4)_3O$ [15]. There is a possibility for Eu^{3+} to substitute La^{3+} in any of the three different sites available. According to Huang and Sleight the Ca(1) and Ca(3) sites have C_3 symmetry and Ca(2) has C_1 symmetry in $BiCa_4(VO_4)_3O$ [13]. This shows that Eu^{3+} is present in La(1) and/or La(3) site(s).

The emission line observed at 579.5 nm is due to $^5D_0 \rightarrow {}^7F_0$ transition which is a forbidden transition. The $^5D_0 \rightarrow {}^7F_0$ transition is observed when Eu^{3+} occupies a site with C_v, C_{nv} or C_s symmetry [23]. The intensity of $^5D_0 \rightarrow {}^7F_0$ transition depends on the nature and strength of Eu^{3+}–O^{2-} bond. Unusual intensity for $^5D_0 \rightarrow {}^7F_0$ transition has been reported when there exists a short and highly covalent bond [15,26–29]. In the present study, the intensity of $^5D_0 \rightarrow {}^7F_0$ transition is less when compared to $^5D_0 \rightarrow {}^7F_{1,2}$ transitions. The relative intensity of $^5D_0 \rightarrow {}^7F_0$ transition decreases with change in alkaline earth ions from Ca to Ba. This result suggests that the covalency of Eu^{3+}–O^{2-} bond decreases with increasing size of the alkaline earth ion. As the counter cation becomes bigger, the O^{2-} ions become less polarized. This results in

Table 2
Assignments (cm^{-1}) of FT-IR spectra

Compound	ν_3 ν_{as}(Si–O)	ν_4 δ(Si–O)
$CaLa_3Bi(SiO_4)_3O$	931	545, 494
$SrLa_3Bi(SiO_4)_3O$	924	541, 491
$BaLa_3Bi(SiO_4)_3O$	914	536, 493
$CaLa_2Bi_2(SiO_4)_3O$	934	546, 492
$SrLa_2Bi_2(SiO_4)_3O$	930	543, 489
$BaLa_2Bi_2(SiO_4)_3O$	915	539, 490

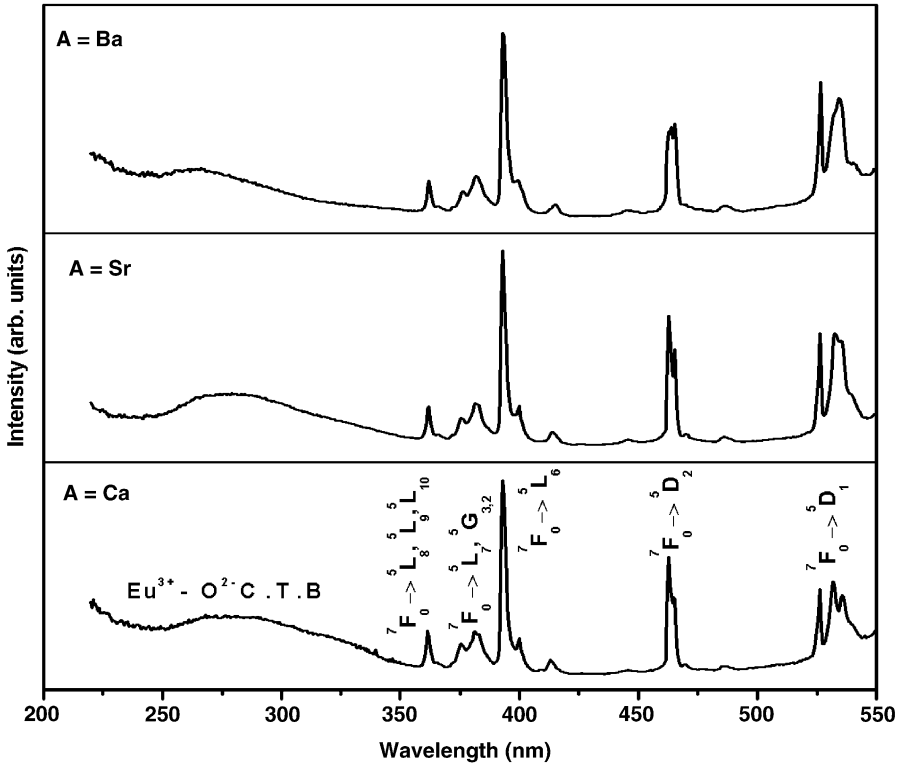

Fig. 6. Photoluminescence excitation spectra of $ALa_{2.95}Eu_{0.05}Bi(SiO_4)_3O$ [A=Ca, Sr and Ba]; $\lambda_{em} = 614$ nm.

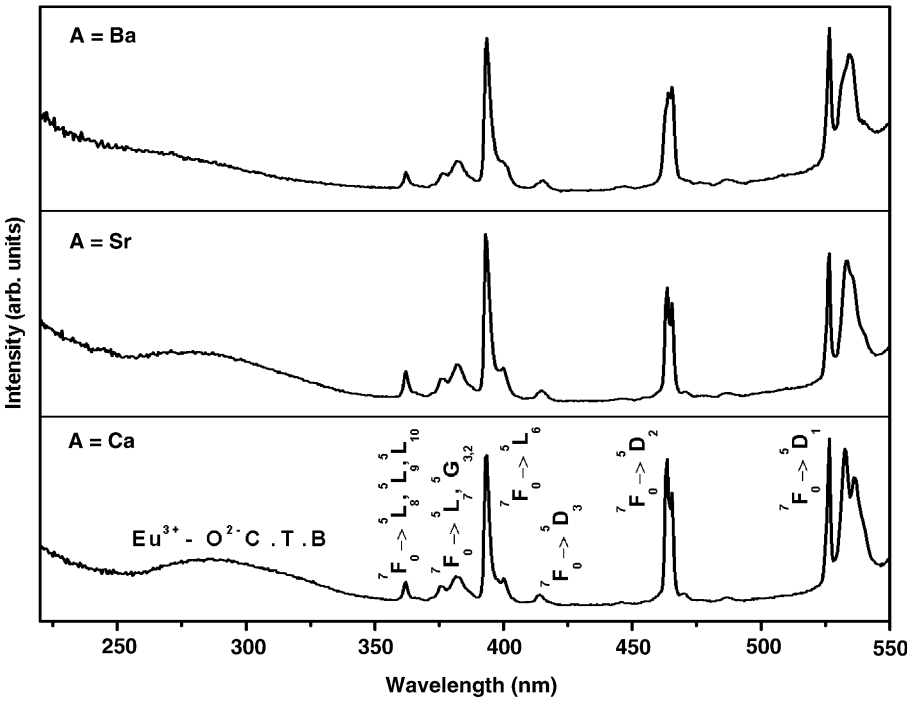

Fig. 7. Photoluminescence excitation spectra of $A La_{1.95}Eu_{0.05}Bi_2(SiO_4)_3O$ [A=Ca, Sr and Ba]; $\lambda_{em} = 614$ nm.

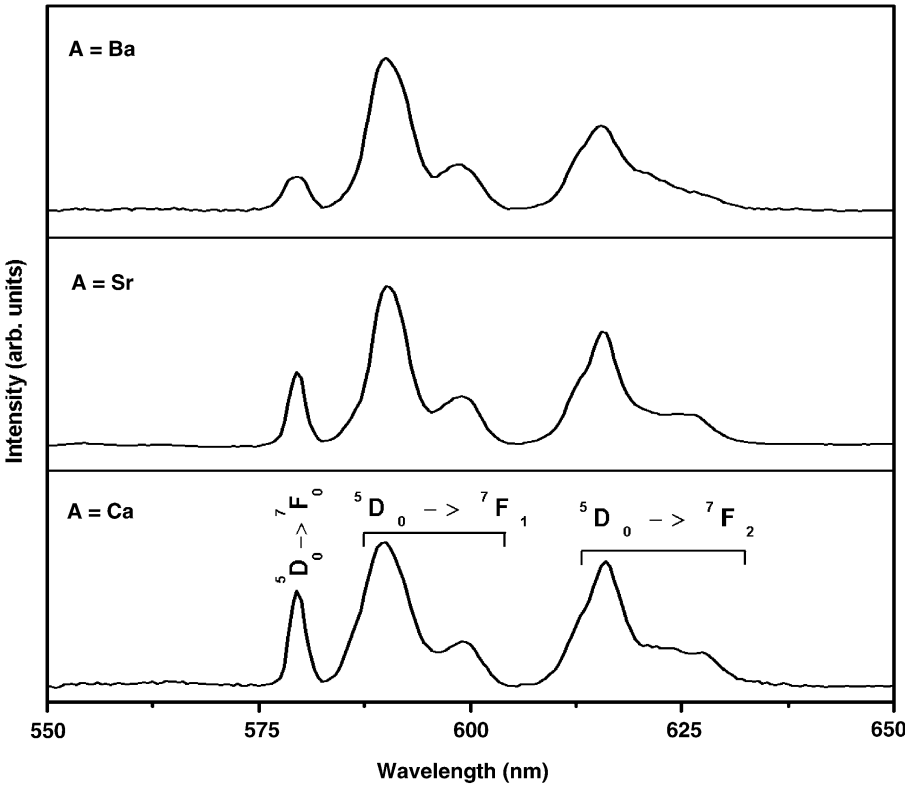

Fig. 8. Photoluminescence emission spectra of $A La_{2.95}Eu_{0.05}Bi(SiO_4)_3O$ [A=Ca, Sr and Ba]; $\lambda_{exc.} = 395$ nm.

the decrease in covalency of Eu^{3+}–O^{2-} bond and so the intensity of $^5D_0 \rightarrow {}^7F_0$ transition. Recent results of Eu^{3+} emission in $BiCa_4(PO_4)_3O$ have shown that the emission line at 579 nm corresponds to $^5D_0 \rightarrow {}^7F_0$ transition and points to the Eu^{3+} in Ca(1) site [15]. Similarly, the emission of $^5D_0 \rightarrow {}^7F_0$ occurs at 579.5 nm in $A La_3Bi(SiO_4)_3O$ and

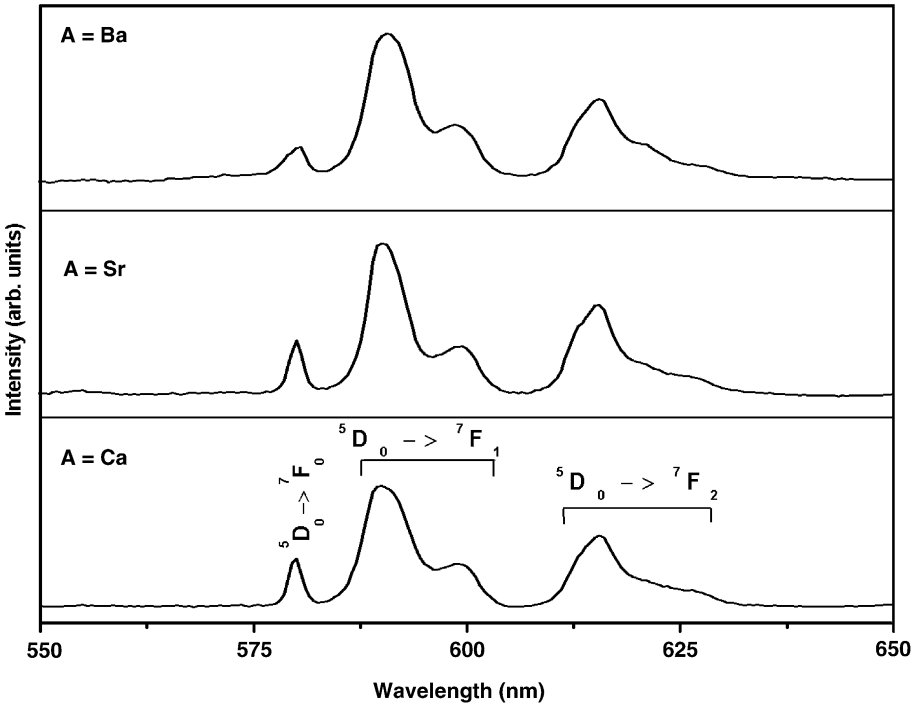

Fig. 9. Photoluminescence emission spectra of ALa$_{1.95}$Eu$_{0.05}$Bi$_2$(SiO$_4$)$_3$O [A=Ca, Sr and Ba]; $\lambda_{exc.} = 395$ nm.

ALa$_2$Bi$_2$(SiO$_4$)$_3$O [A=Ca, Sr and Ba] and this can be attributed to Eu^{3+} present in La(1) site. The presence of single emission line for $^5D_0 \rightarrow {}^7F_0$ transition suggests that Eu^{3+} is present in only one site. The observed Eu^{3+} emission results in the present study are entirely different from the results reported in silicate oxyapatites in the literature [10,24,30]. This reveals that the compounds ALa$_3$Bi(SiO$_4$)$_3$O and ALa$_2$Bi$_2$(SiO$_4$)$_3$O [A=Ca, Sr and Ba] differ from the ideal apatite structure and their relation to BiCa$_4$(VO$_4$)$_3$O which has an apatite-related structure is more ideal.

4. Conclusions

New oxysilicates with the general formula ALa$_3$Bi(SiO$_4$)$_3$O and ALa$_2$Bi$_2$(SiO$_4$)$_3$O [A=Ca, Sr and Ba] are reported for the first time. The broad emission lines of Eu^{3+} in the newly synthesized oxysilicates reveal the disorder of cations. The relatively high intense magnetic dipole transition $^5D_0 \rightarrow {}^7F_1$ points to a more symmetric environment which is normally not observed in apatites. This confirms that the structural relationship of the oxysilicates synthesized in the present study with apatite-related BiCa$_4$(VO$_4$)$_3$O is more appropriate.

Acknowledgments

The author N. Lakshminarasimhan acknowledges the Council of Scientific and Industrial Research (CSIR), New Delhi for research fellowship.

References

[1] K. Sudarsanan, P.E. Mackie, R.A. Young, Mater. Res. Bull. 7 (1972) 1331–1338.
[2] P.E. Mackie, J.C. Elliott, R.A. Young, Acta Crystallogr. B 28 (1972) 1840–1848.
[3] P.R. Suitch, A. Taitai, J.L. Lacout, R.A. Young, J. Solid State Chem. 63 (1986) 267–277.
[4] J.E.H. Sansom, D. Richings, P.R. Slater, Solid State Ion. 139 (2001) 205–210.
[5] L.M. Rodríguez-Lorenzo, J.N. Hart, K.A. Gross, J. Phys. Chem. B 107 (2003) 8316–8320.
[6] T.S. Davis, E.R. Kreidler, J.A. Parodi, T.F. Soules, J. Lumin. 4 (1971) 48–62.
[7] L.L. Reina, M.C.M. Sedeño, E.R. Losilla, A. Cabeza, M.M. Lara, S. Bruque, F.M.B. Marques, D.V. Sheptyakov, M.A.G. Aranda, Chem. Mater. 15 (2003) 2099–2108.
[8] J. Ito, Am. Mineral. 53 (1968) 890–906.
[9] J. Felsche, J. Solid State Chem. 5 (1972) 266–275.
[10] T.J. Isaacs, J. Electrochem. Soc. 120 (1973) 654–656.
[11] G. Blasse, J. Solid State Chem. 14 (1975) 181–184.
[12] T.J. White, D. ZhiLi, Acta Crystallogr. B 59 (2003) 1–16.
[13] J. Huang, A.W. Sleight, J. Solid State Chem. 104 (1993) 52–58.
[14] G. Buvaneswari, U.V. Varadaraju, J. Solid State Chem. 149 (2000) 133–136.
[15] N. Lakshminarasimhan, U.V. Varadaraju, J. Solid State Chem. 177 (2004) 3536–3544.
[16] J.R. Tolchard, J.E.H. Sansom, P.R. Slater, M.S. Islam, J. Solid State Electrochem. 8 (2004) 668–673.
[17] K. Yvon, W. Jeitschko, E. Parthe, J. Appl. Crystallogr. 10 (1977) 73–74.
[18] K. Nakamoto, Infrared and Raman Spectra of Inorganic and Coordination Compounds, fifth ed, Wiley, New York, 1997.
[19] L. Boyer, J. Carpena, J.L. Lacout, Solid State Ion. 95 (1997) 121–129.

[20] D. Arcos, J. Rodríguez-Carvajal, M. Vallet-Regí, Chem. Mater. 17 (2005) 57–64.
[21] G. Blasse, J. Solid State Chem. 4 (1972) 52–54.
[22] G. Blasse, A. Bril, J. Inorg. Nucl. Chem. 29 (1967) 2231–2241.
[23] G. Blasse, A. Bril, Philips Res. Repts. 21 (1966) 368–378.
[24] L. Boyer, B. Piriou, J. Carpena, J.L. Lacout, J. Alloys. Compd. 311 (2000) 143–152.
[25] G. Blasse, A. Bril, W.C. Nieuwpoort, J. Phys. Chem. Solids. 27 (1966) 1587–1592.
[26] B. Piriou, D. Fahmi, J. Dexpert-Ghys, A. Taitai, J.L. Lacout, J. Lumin. 39 (1987) 97–103.
[27] A.M. Pires, M.R. Davolos, O.L. Malta, J. Lumin. 72–74 (1997) 244–246.
[28] B. Piriou, M. Richard-Plouet, J. Parmentier, F. Ferey, S. Vilminot, J. Alloys Compd. 262–263 (1997) 450–453.
[29] B. Piriou, Y.F. Chen, S. Vilminot, Eur. J. Solid State Inorg. Chem. 35 (1998) 341–355.
[30] Q. Su, J. Lin, B. Li, J. Alloys. Compd. 225 (1995) 120–123.